Multiple image storage and frequency conversion in a cold atomic ensemble

Dong-Sheng Ding,* Jing-Hui Wu, Zhi-Yuan Zhou, Bao-Sen Shi,† Xu-Bo Zou, and Guang-Can Guo
Key Laboratory of Quantum Information, University of Science and Technology of China, Hefei 230026, China
(Received 30 August 2012; revised manuscript received 14 February 2013; published 24 May 2013)

The strong demand for quantum memory, a key building block of quantum network, has inspired new methodologies and led to experimental progress for quantum storage. The use of quantum memory for spatial multimode or image storage could dramatically increase the channel bit rate. Furthermore, quantum memory that can store multiple optical modes would lead to higher efficiencies in quantum communication and computation. Here, by using resonant tripod electromagnetically induced transparency in a cold atomic ensemble, we experimentally demonstrate the storage of two probes with different frequencies and images in the frequency domain. In addition, by using different read light, we realize the frequency conversion of retrieved images with high efficiency. Besides, our method may be used to create a superposition of the images by realizing the function of a beam splitter. All advantages make our method useful in many fields, including quantum information, detection, imaging, sensing, and so on.

DOI: 10.1103/PhysRevA.87.053830 PACS number(s): 42.50.Gy, 42.65.Hw

I. INTRODUCTION

A long-distance quantum communication network consists of a memory in which quantum information can be stored and manipulated and a carrier via which the different memories could connect with others. The seminal work of Duan *et al.* [1] shows that an atomic system may be a suitable candidate for the memory and a photon could be a robust and efficient carrier due to its weak interaction with the environment.

The strong demand for quantum memory has inspired new methodologies, leading to experimental progress for quantum storage via different mechanisms in an atomic system, for example, via electromagnetically induced transparency (EIT) [2,3], atomic frequency combs [4,5], Raman schemes [6,7], gradient echo technique [8,9], etc. Even so, there has been little progress on spatial multimode or image storage.

A quantum memory which could store spatial multimodes or images is very useful because it could dramatically increase the channel bit rate. Recently, there has been some progress related to the storage of images, for example, works via EIT in a hot atomic ensemble [10,11] or a cryogenically cooled doped solid [12], experiments using the four-wave mixing technique in a hot [13] or cold atomic ensemble [14], and the report using a gradient echo memory in a hot atomic ensemble [15]. Additionally, quantum memories that are able to store multiple optical modes offer advantages over single-mode memories in terms of speed and robustness, leading to higher efficiencies in quantum communication and computation experiments [16,17]. There have been some experimental reports in this direction. In Ref. [8], a multimode structure in the time domain is stored via the gradient echo technique in a hot atomic ensemble; in Ref. [4], an atomic frequency comb is applied to store multimodes in the time domain too. Very recently, we reported the experimental storage of two different images in the spatial domain through EIT in a cold ^{85}Rb atomic cloud [18].

A promising way of storing multiple optical modes is to store the different optical modes in different atomic collective spin excitation states, which could, for example, be realized by a tripod configuration of atoms. There has been some related progress (no image) along this direction [19,20]. In this paper, we report experimental evidence that two different images can be stored using EIT in a tripod configuration in a cold atomic ensemble. The development of multimode quantum image memories should be an important step towards the realization of high-dimensional quantum networks. Furthermore, by using different read light, we realize the highly efficient frequency conversion of the stored images. It is about 3 orders higher than that achieved in a recent up-conversion experiment by the four-wave mixing in a hot atomic ensemble [21,22]. Although the wavelength difference between the input image and the converted image is only about 15 nm in our experiment, the frequency conversion of images between different wavelength bands could be realized by selecting suitable atomic energy levels or a suitable atom. The image conversion could be realized in a hot atomic ensemble too; therefore, the whole experimental system could be much simplified and miniaturized. We believe that such a technique would find wide applications in detection, imaging, sensing, and even astrophysical observation [23–26]. In Ref. [27], Yu *et al.* report the frequency conversion of a stored light using a different retrieve light, but they only consider the light without any spatial information. Besides, we could create the superposition of the two images by realizing the function of a beam splitter, which is a key element of quantum information processing. The big difference in this respect compared with previous reported work [28] is that we could create the superposition of images.

We consider the state of input probe fields being expressed below:

$$|\psi_{\text{input}}\rangle = |\lambda_1\rangle|I_1\rangle + |\lambda_1'\rangle|I_2\rangle, \tag{1}$$

where, λ_1, λ_1' indicates wavelength, $I_{1,2}$ describes spatial information, $|\lambda_1\rangle|I_1\rangle$ and $|\lambda_1'\rangle|I_2\rangle$ describe input probes 1 and 2 with wavelengths λ_1 and λ_1', respectively. The frequency shift

*Corresponding author: dds@mail.ustc.edu.cn
†drshi@ustc.edu.cn

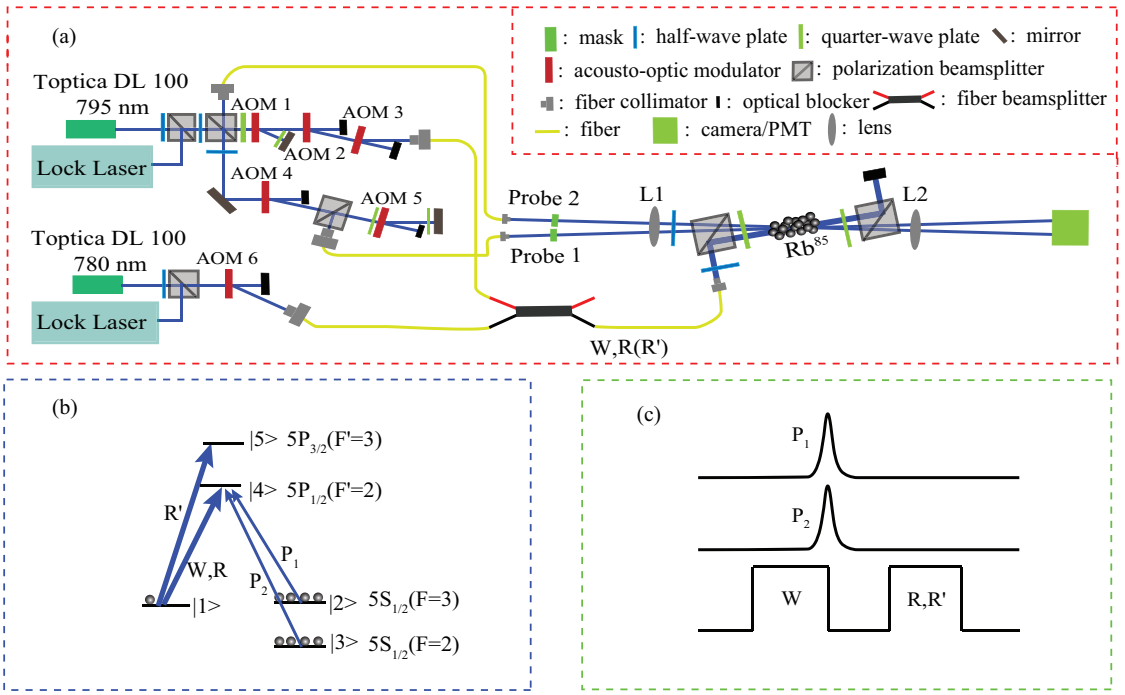

FIG. 1. (Color online) (a) Experimental setup. The frequency of probe 1 (P_1) is shifted by AOM 4 (frequency shift 160 MHz) and AOM 5 (double-pass frequency shift −160 MHz). The frequency of probe 2 (P_2) is shifted by AOM 1 (double-pass frequency shift 3.0378 GHz). The frequency of W or R is shifted by AOM 2 (frequency shift 80 MHz) and AOM 3 (frequency shift − 80 MHz). The read beam R' is modulated by AOM 6. (b) Experimental energy diagram. (c) Timing sequence. Probe fields are modulated by acoustic-optical modulators to form a Gaussian pulse sequence. The W field writes the probe fields into the atomic collective spin excitation states and the R, R' fields read them out.

between these two probe fields is defined as Δ. If we use the λ_1 field as read light, then the retrieved probe 1, 2 fields are expressed as

$$|\psi_{\text{output}}\rangle = \sqrt{\eta_1}|\lambda_1\rangle|I_1\rangle + \sqrt{\eta_2}|\lambda_1'\rangle|I_2\rangle, \tag{2}$$

where $\sqrt{\eta_1}|\lambda_1\rangle|I_1\rangle$ describes the retrieved probe 1 at λ_1 with storage efficiency of η_1 and $\sqrt{\eta_2}|\lambda_1'\rangle|I_2\rangle$ corresponds to the retrieved probe 2 at λ_1' with storage efficiency of η_2. If we apply a λ_2 field as read light, then the readout probe fields can be described by

$$|\psi_{\text{output}}\rangle = \sqrt{\eta_3}|\lambda_2\rangle|I_1\rangle + \sqrt{\eta_4}|\lambda_2'\rangle|I_2\rangle, \tag{3}$$

where $\sqrt{\eta_3}|\lambda_2\rangle|I_1\rangle$ describes the retrieved probe 1 at λ_2 with conversion efficiency of η_3 and $\sqrt{\eta_4}|\lambda_2'\rangle|I_2\rangle$ corresponds to the retrieved probe 2 at λ_2' with conversion efficiency of η_4. The frequency shift between λ_2 and λ_2' is still Δ. The frequencies

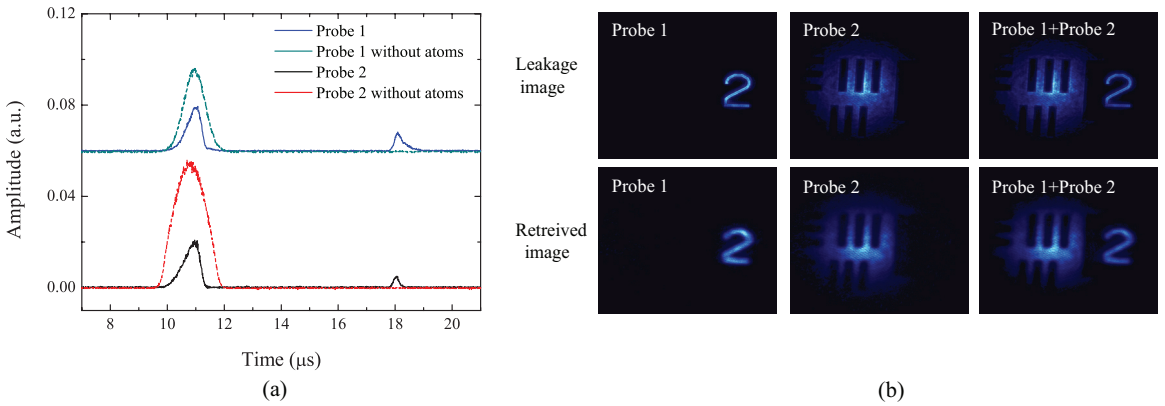

FIG. 2. (Color online) (a) The intensities of the leakage and retrieved probe fields recorded by two PMTs. The green dotted line (top) is probe 1 without atoms and the blue solid line (top) is the storage of probe 1. The red dotted line (bottom) is probe 2 without atoms and the black solid line (bottom) is the storage of probe 2. (b) The leakage and retrieved images recorded by CCD. Each image is the sum of the 50 retrieved images. The exposure time of the CCD camera was 1.0 s. Probes 1 and 2 are stored for about 6.7 μs. The power of the W or R field is 100 μW and the R' field is 140 μW. The photon number of each probe is about 2.7×10^4.

of retrieved probes are changed in comparison with Eq. (2); therefore, the frequency conversion of the stored image is realized.

II. EXPERIMENTAL CONFIGURATION

Figure 1(a) shows the schematic experimental setup. A tripod configuration shown in Fig. 1(b) was used to perform the storage experiment. A cigar-shaped atomic cloud of ^{85}Rb atoms, trapped in a two-dimensional magneto-optical trap (MOT), was used as the storing medium. The size of cloud was about $30 \times 2 \times 2$ mm^3. The total atom number was 9.1×10^8 [29]. The probe fields (probe 1 and 2) and the write (W) or read (R) beam from an external-cavity diode laser (ECDL, DL100, Toptica) had the same wavelength of 795 nm. The probe fields were imprinted a real image through a standard resolution chart (USAF target). The other read (R') beam from another ECDL has the wavelength of 780 nm. Probe 1 (P_1) and the W or R fields are resonant with the transitions of $5S_{1/2}(F=3, m_F=-3)(|2\rangle) - 5P_{1/2}(F'=2, m_F=-2)(|4\rangle)$ and $5S_{1/2}(F=3, m_F=-1)(|1\rangle) - 5P_{1/2}(F'=2, m_F=-2)(|4\rangle)$, respectively. Probe 2 (P_2) is resonant with the transition of $5S_{1/2}(F=2, m_F=-2)(|3\rangle) - 5P_{1/2}(F'=2, m_F=-2)(|4\rangle)$. The R' field is resonant with the transition of $5S_{1/2}(F=3, m_F=-1)(|1\rangle) - 5P_{3/2}(F'=3, m_F=-2)(|5\rangle)$. P_1 and P_2 have the same linear polarizations and copropagate with a small angle of 0.1°. The angle between P_1 and the read beam is about 2.5°; their polarizations are orthogonal. The W, R, and R' beams have the same linear polarizations. The noncollinear configuration used in the experiment significantly reduces the noise from the scattering of the write or read light. We used two photomultiplier tubes (PMTs) (Hamamatsu, H10721) to detect the intensities of probe fields in the time domain and used a time-resolution camera (CCD, 1024×1024, iStar 334T series, Andor) to monitor spatial structure. By adjusting a quarter-wave plate before the MOT, the write or read and probe fields were assigned opposite circular polarizations. Using a quarter-wave plate after the MOT, the fields were later reversed to have orthogonal linear polarizations.

III. EXPERIMENTAL RESULTS

We take the experimental parameters to be as follows: $\lambda_1 = 795$ nm, $\lambda_1' = 795$ nm (the frequency shift between them is $\Delta = 3.0378$ GHz); I_1 and I_2 describe the spatial information of the digit "2" and the frame image, respectively. The wavelength of R is $\lambda_1 = 795$ nm. The W or R field and the R' field are 3 mm in diameter and cover probe beams completely. If we use the R field as read light, the retrieved signals have a wavelength of 795 nm. The signals detected by PMTs are shown in Fig. 2(a). The storage efficiency of probe 1 is $\eta_1 = 0.098$; the storage efficiency of probe 2 is $\eta_2 = 0.023$. Here the storage efficiency is defined as the ratio between the areas under the retrieved probe profile and the input probe's without atoms. Then, we change the PMTs to CCD for detecting spatial information. The retrieved images are shown in Fig. 2(b). The left column corresponds to the storage of probe 1 and the middle column to the storage of probe 2. The case of probes 1 and 2 being simultaneously stored and retrieved is shown in the right column of Fig. 2(b). There is almost no difference between the leakage images and the retrieved images. We calculate the similarity R of the retrieved images compared with the leakage images in the case of probes 1 and 2 being simultaneously stored and retrieved using the formula $R = \frac{\sum_m \sum_n A_{mn} B_{mn}}{\sqrt{\sum_m \sum_n A_{mn}^2 \sum_m \sum_n B_{mn}^2}}$, where A_{mn} and B_{mn} are the grayscale intensities recorded for pixels m and n of the two images to be compared, which is 96%. We also experimentally demonstrate that there is no cross talk between the storage of probe 1 and probe 2. The detailed experimental results are shown later.

Next, we want to see what will happen if a different read light R' with a different wavelength is used. In order for that to occur, we use the R' field with the wavelength of $\lambda_2 = 780$ nm as the read light; the results in time domain are shown in Fig. 3(a). The leakage signals have a wavelength of 795 nm,

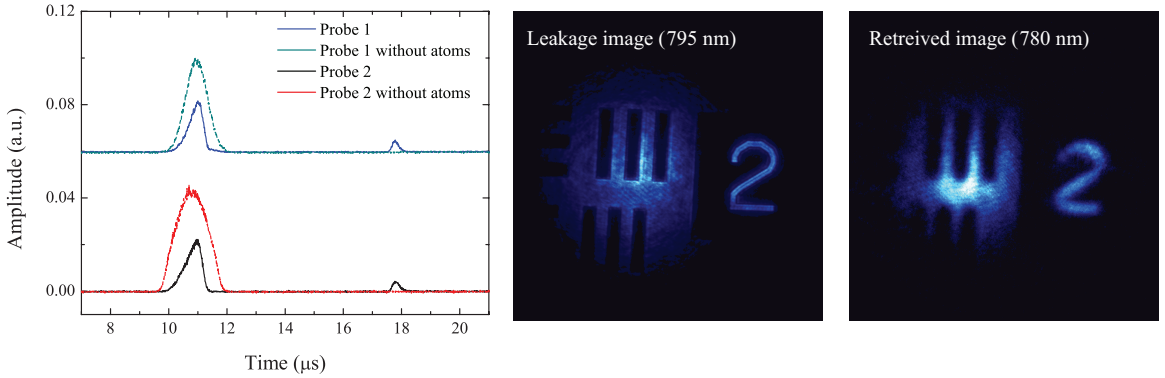

FIG. 3. (Color online) (a) The intensity signal in the time domain recorded by PMTs. The green dotted line (top) is probe 1 without atoms and the blue solid line (top) is the storage of probe 1. The red dotted line (bottom) is probe 2 without atoms and the black solid line (bottom) is the storage of probe 2. The storage time of probe fields is about 6.7 μs. The left panel of (b) is the leakage image with a wavelength of 795 nm; the right panel is the retrieved image with a wavelength of 780 nm. Each image is the sum of the 50 retrieved images. The exposure time of the CCD camera was 1.0 s. The image storage time is about 6.7 μs. The power of the W or R field is 100 μW and the R' field is 140 μW. The photon number of each probe is about 2.7×10^4.

but the retrieved signals have a wavelength of 780 nm. The frequency conversion efficiency of probe 1 is $\eta_3 = 0.017$; the efficiency of probe 2 is $\eta_4 = 0.018$. Here the conversion efficiency is defined as the ratio between the areas under the retrieved probe profile and the input probe's without atoms. Figure 3(b) is a record of the spatial structures of retrieved probes using CCD. The experimental results show that the frequency of the output fields can be changed using different read light and the spatial information of the probe field could still be preserved. We also calculate the similarity R of the retrieved images compared with the leakage images in the case of probes 1 and 2 being simultaneously stored and converted, as shown Fig. 3(b), which is about 99%. Therefore, we realize the image storage and its frequency conversion simultaneously in a single storage device. We also find that the efficiency of conversion decreases with the increase of the angle between the probes and the write or read light.

Then we try to answer the question of whether there is cross talk between the stored images. Experimentally, we check the cross talk against the angle between the write or read and probe fields, where the probes have different frequencies. The angle between the write or read and probe 1 is defined as α; the angle between the probes 1 and 2 is defined as β. We keep the angle of β being 0.5° unchanged first and check the cross talk against the change of the angle α. The experimental results are shown in Fig. 4. The left column in the each picture is for probe 1, the middle column is for probe 2, and the right column is for probe 1 + 2. Each picture is the extract from the background. The top line in each picture is a leaked image and the bottom line corresponds to the retrieval. In this process, the

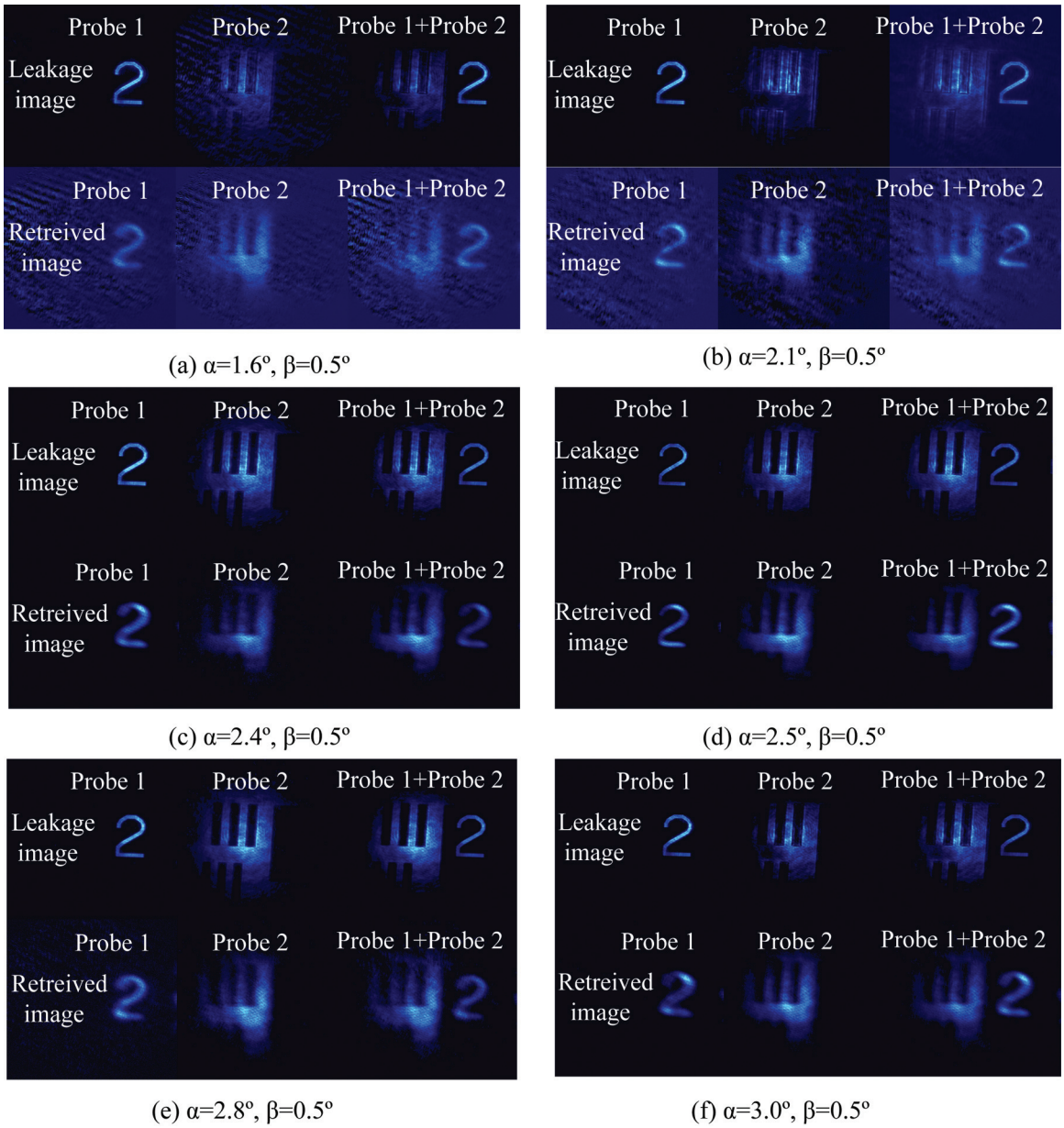

FIG. 4. (Color online) The cross talk between the images against the angle between α. The angle β is kept to be $\beta = 0.5^\circ$ in all measurements. When α is small, the noise from the W or R field is difficult to reduce, so panels (a) and (b) have little blur.

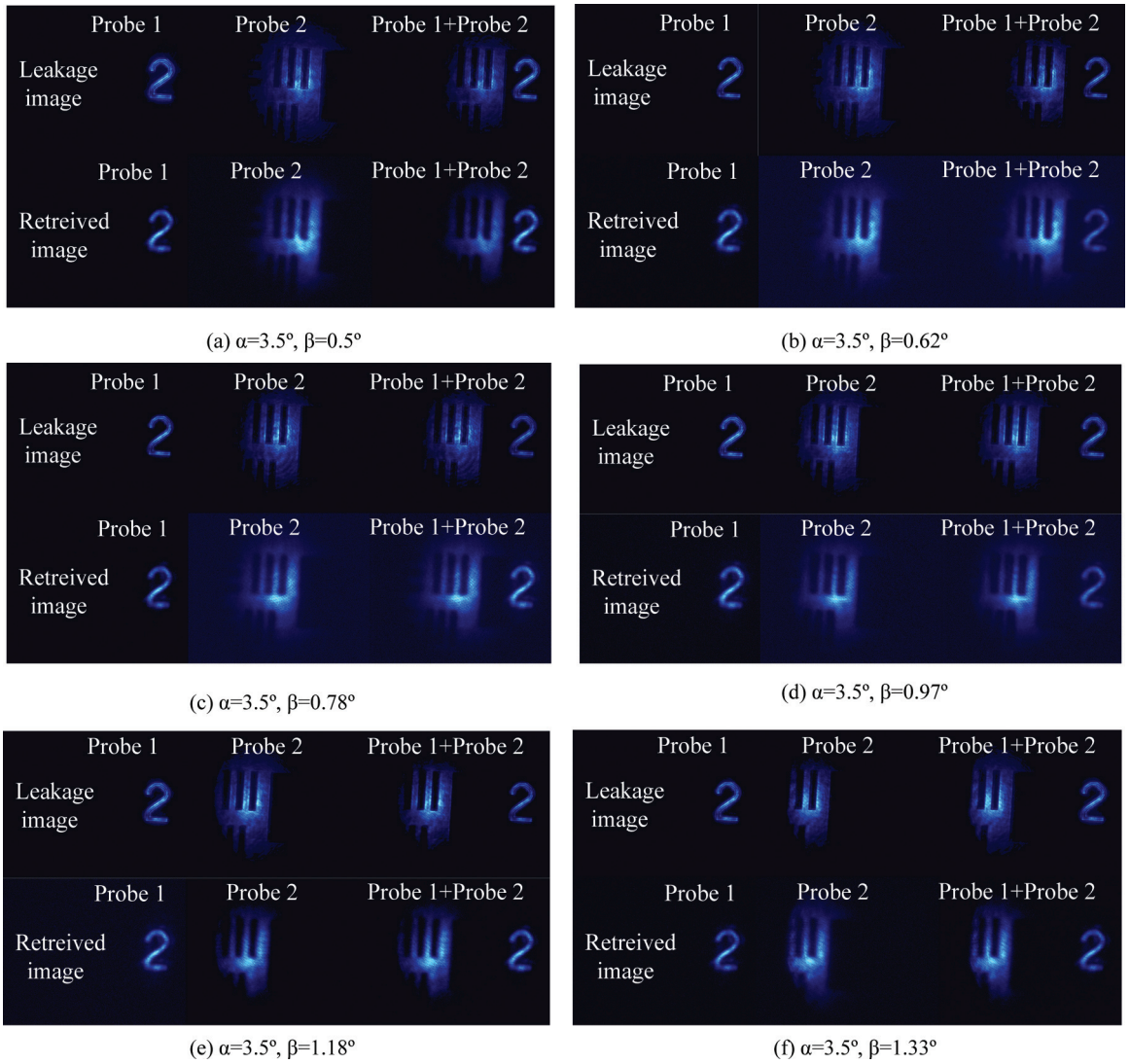

(a) α=3.5°, β=0.5°

(b) α=3.5°, β=0.62°

(c) α=3.5°, β=0.78°

(d) α=3.5°, β=0.97°

(e) α=3.5°, β=1.18°

(f) α=3.5°, β=1.33°

FIG. 5. (Color online) The cross talk between the images against the angle of β. The angle of α is kept to be 3.5° in all measurements.

storage time is about 7 μs. Obviously, there is also no cross talk in this situation.

Then we keep the angle of α being 3.5° unchanged and check the cross talk against the change of the angle β. In our experiment, when the angle is larger than 1.33°, the camera cannot collect both probes simultaneously. If the angle β is too small, the two images are overlapped. Therefore, we only change the angle between $\beta = 0.5°$ and $\beta = 1.33°$. In this process, the storage time is about 7 μs. The experimental results are shown in Fig. 5. It clearly shows that there is no cross talk between the stored images either.

A potential interesting question is what would happen if two images are stored overlapping? Does the retrieved light contain an interesting pattern? Or is the intensity simply added? We perform the storage experiments under two different conditions to answer these questions. In order to simplify the experiment, we only consider the storages of probes without images. In situation 1, probes 1 and 2 have different frequencies. Probe 1 is resonant on the transition $5S_{1/2}(F = 3)(|2\rangle) - 5P_{1/2}(F' = 2)(|4\rangle)$; probe 2 is resonant on the transition $5S_{1/2}(F = 2)(|3\rangle) - 5P_{1/2}(F' = 2)(|4\rangle)$. In situation 2, probes 1 and 2 have the same frequencies and are all resonant on the transition $5S_{1/2}(F = 3)(|2\rangle) - 5P_{1/2}(F' = 2)(|4\rangle)$. In these two cases, R read (795-nm laser) light is used to read the stored probes 1 and 2 out. The results are shown in Fig. 6. The retrieved interference phenomenon is observed only under the condition that the probes 1 and 2 have same frequency. In situation 1, we could not observe the interference pattern due to the large frequency difference (3 GHz) between probes. The results we obtained clearly demonstrate that the storage is coherent. By plotting the intensity profiles in the horizontal direction through the center of the interference pattern, we calculated the visibilities of the leaked and retrieved images using the formula $V = \frac{I_{\max} - I_{\min}}{I_{\max} + I_{\min}}$, where $I_{\max}$ and $I_{\min}$ were the maximal and minimal photon counts along the horizontal direction of the interference pattern, which are 75% and 71%, respectively.

IV. DISCUSSION AND ANALYSIS

In Fig. 3, there are about 2.7×10^4 photons per pulse being stored, which is higher than the number of photons per

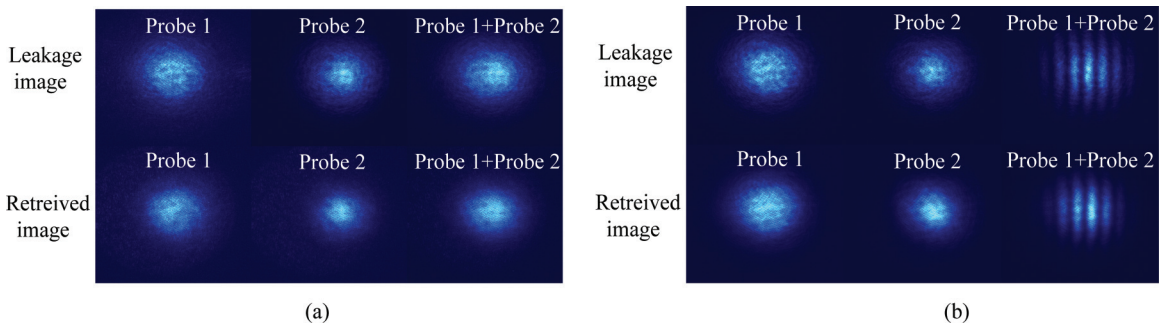

FIG. 6. (Color online) The storage under the condition of overlapping of probes 1 and 2. (a) Probes 1 and 2 have a 3.0-GHz frequency difference. (b) Probes 1 and 2 have same frequencies.

pulse in Ref. [18]. In this experiment, the atomic populations of energy levels $|2\rangle$ and $|3\rangle$ in this tripod configuration are relatively small compared with the degenerate configuration in Ref. [18]. Then, the storage efficiency is lower compared with the degenerate configuration. In Figs. 3 and 4, we observe that the input state $|\psi_{\text{input}}\rangle = \sum |\lambda_i\rangle|I_j\rangle$ is converted into the state $|\psi_{\text{output}}\rangle = \sum \sqrt{\eta_n}|\lambda_n\rangle|I_j\rangle$, where $(n,i,j) = (1,2)$. This process can be used to realize the function of a beam splitter, by which the superposition of the different images at different wavelengths is obtained. This function can be realized by storing only part of the probes, such that the leakage image and the retrieved image consist of the superposition. We could realize two different superposition images states: One is the superposition state of the leaked part and the retrieved part without frequency conversion; another is the superposition state consisting of the leaked part with wavelength of λ_1 and the retrieved part with the wavelength of λ_2 with the frequency conversion. It is worth illustrating that efficiency of the frequency conversion is much higher than that achieved through a four-wave mixing in an atomic system. The frequency conversion in this work is essentially a four-wave mixing, a process which is split into two delayed parts, with a long-lived coherence in the atoms connecting the storage and retrieval processes. The atoms are coherently prepared during the process of storage. It has been demonstrated previously that coherently prepared media may enhance nonlinear optical interaction [30,31]. Therefore, the efficiency is much higher compared with other works. Although the wavelength difference between the input image and the converted image is only about 15 nm in our experiment, we could realize the frequency conversion of images between different wavelength bands by selecting suitable atomic energy levels or selecting a suitable atom. For example, if the energy level of $6p$ of the ^{85}Rb atom is considered, then the image could be transferred from a light in the near infrared band (795 nm) to a light in the ultraviolet band (420 nm) or vice versa. Although our experiment was done in a cold atomic ensemble, it could be realized in a hot atomic ensemble; therefore, the whole experimental system could be much simplified and miniaturized.

Although the storage of two images by means of frequency multiplexed EIT in the tripod configuration is done in classical region, it may be workable in quantum region. In order for that, the signal-to-noise ratio (SNR) should be improved greatly. We think one main noise source is the scattering of the read light when we switch it on. Fortunately, such noise could be reduced significantly by using a noncollinear EIT configuration, as done in our present experiments. We have found that with the increase of the angle between the probe and the read pulses, the noise reduces gradually. In principle, we might further increase the angle further, but it would reduce the EIT dip and result in a decrease in memory efficiency. Therefore, we had to reach a compromise between the angle and the achievable efficiency. The second noise source is from the dephasing between two ground states induced by Earth's magnetic field and the atomic motion. It not only reduces the SNR, but also shortens the storage time. Another noise source is from the environment of our laboratory. The lights from the liquid crystal indicators or indicator lamps of all kinds of equipments would also contribute to the dark counts of the CCD camera. Besides, the large sensor area of the CCD camera (13.3×13.3 mm^2) also records more noise photons. All the noise sources together make our scheme unworkable at the single-photon level at present.

V. CONCLUSION

In summary, we have experimentally demonstrated that multiple images can be stored and retrieved in a cold atomic ensemble using resonant tripod EIT configuration. The probe fields can be converted to different frequencies by applying different read light while the spatial information is preserved. Our results are important for future quantum communication in high-dimensional quantum networks and other fields.

Note added in proof. Recently, we noticed a parallel work [32], in which, the gradient photon echo technique was used to realize the storage of multiple images in a hot atomic ensemble.

ACKNOWLEDGMENTS

This work was supported by the National Natural Science Foundation of China (Grants No. 11174271, No. 61275115, and No. 10874171), the National Fundamental Research Program of China (Grant No. 2011CB00200), and the Innovation fund from CAS, Program for NCET.

[1] L.-M. Duan, M. D. Lukin, J. I. Cirac, and P. Zoller, Nature (London) **414**, 413 (2001).
[2] M. Fleischhauer and M. D. Lukin, Phys. Rev. Lett. **84**, 5094 (2000).
[3] D. F. Phillips, M. Fleischhauer, A. Mair, R. L. Walsworth, and M. M. Lukin, Phys. Rev. Lett. **86**, 783 (2001).
[4] M. Afzelius, C. Simon, H. de Riedmatten, and N. Gisin, Phys. Rev. A **79**, 052329 (2009).
[5] H. de Riedmatten, M. Afzelius, M. U. Staudt, C. Simon, and N. Gisin, Nature (London) **456**, 773 (2008).
[6] R. F. Reim, P. Michelberger, K. C. Lee, J. Nunn, N. K. Langford, and I. A. Walmsley, Phys. Rev. Lett. **107**, 053603 (2011).
[7] K. F. Reim, J. Nunn, V. O. Lorenz, B. J. Sussman, K. C. Lee, N. K. Langford, D. Jaksch, and I. A. Walmsley, Nat. Photon. **4**, 218 (2010).
[8] M. Hosseini, B. M. Sparkes, G. Campbell, P. K. Lam, and B. C. Buchler, Nat. Comm. **2**, 174 (2011).
[9] M. Hosseini, G. Campbell, B. M. Sparkes, P. K. Lam, and B. C. Buchler, Nat. Phys. **7**, 794 (2011).
[10] P. K. Vudyasetu, R. M. Camacho, and J. C. Howell, Phys. Rev. Lett. **100**, 123903 (2008).
[11] M. Shuker, O. Firstenberg, R. Pugatch, A. Ron, and N. Davidson, Phys. Rev. Lett. **100**, 223601 (2008).
[12] G. Heinze, A. Rudolf, F. Beil, and T. Halfmann, Phys. Rev. A **81**, 011401(R) (2010).
[13] A. M. Mariuno, R. C. Pooser, V. Boyer, and P. D. Lett, Nature (London) **457**, 859 (2009).
[14] J. Wu, Y. Liu, D. Ding, Z. Zhou, B. Shi, and G. Guo, Phys. Rev. A **87**, 013845 (2013).
[15] D. B. Higginbottom, B. M. Sparkes, M. Rancic, O. Pinel, M. Hosseini, P. K. Lam, and B. C. Buchler, Phys. Rev. A **86**, 023801 (2012).
[16] N. Sangouard, C. Simon, B. Zhao, Y.-A. Chen, H. de Riedmatten, J.-W. Pan, and N. Gisin, Phys. Rev. A **77**, 062301 (2008).
[17] C. Simon, H. de Riedmatten, M. Afzelius, N. Sangouard, H. Zbinden, and N. Gisin, Phys. Rev. Lett. **98**, 190503 (2007).
[18] Dong-Sheng Ding, Jing-Hui Wu, Zhi-Yuan Zhou, Yang Liu, Bao-Sen Shi, Xu-Bo Zou, and Guang-Can Guo, Phys. Rev. A **87**, 013835 (2013).
[19] Shujing Li, Zhongxiao Xu, Haiyan Zheng, Xingbo Zhao, Yuelong Wu, Hai Wang, Changde Xie, and Kunchi Peng, Phys. Rev. A **84**, 043430 (2011).
[20] Hai Wang, Shujing Li, Zhongxiao Xu, Xingbo Zhao, Lijun Zhang, Jiahua Li, Yuelong Wu, Changde Xie, Kunchi Peng, and Min Xiao, Phys. Rev. A **83**, 043815 (2011).
[21] Dong-Sheng Ding, Zhi-Yuan Zhou, Wen Huang, Bao-Sen Shi, Xu-Bo Zou, and Guang-Can Guo, Phys. Rev. A **86**, 033803 (2012).
[22] Dong-Sheng Ding, Zhi-Yuan Zhou, Bao-Sen Shi, Xu-Bo Zou, and Guang-Can Guo, Phys. Rev. A **85**, 053815 (2012).
[23] S. Baldeli, Nat. Photon. **5**, 75 (2011).
[24] M. M. Abbas, T. Kostiuk, and K. W. Ogilvie, Appl. Opt. **15**, 961 (1976).
[25] M. Imaki and T. Kobayashi, Opt. Lett. **32**, 1923 (2007).
[26] M. A. Albota and F. N. C. Wong, Opt. Lett. **29**, 1449 (2004).
[27] Y. W. Lin, W. T. Liao, T. Peters, H. C. Chou, J. S. Wang, H. W. Cho, P. C. Kuan, and I. A. Yu, Phys. Rev. Lett. **102**, 213601 (2009).
[28] K. F. Reim, J. Nunn, X.-M. Jin, P. S. Michelberger, T. F. M. Champion, D. G. England, K. C. Lee, N. K. Langford, and I. A. Walmsley, Phys. Rev. Lett. **108**, 263602 (2012).
[29] Y. Liu, J.-H. Wu, B.-S. Shi, and G.-C. Guo, Chin. Phys. Lett. **29**, 024205 (2012).
[30] R. M. Camacho, P. K. Vudyasetu, and J. C. Howell, Nat. Photon. **3**, 103 (2009).
[31] M. D. Lukin, P. R. Hemmer, and M. O. Scully, Adv. At. Mol. Opt. Phys. **42**, 347 (2000).
[32] Quentin Glorieux, Jeremy B. Clark, Alberto M. Marino, Zhifan Zhou, and Paul D. Lett, Opt. Express **20**, 12350 (2012).